applied sciences

MDPI

Article

A Bilateral Craniectomy Technique for In Vivo Photoacoustic Brain Imaging

Laura S. McGuire [1], Mohsin Zafar [2], Rayyan Manwar [2], Fady T. Charbel [1] and Kamran Avanaki [2,*]

[1] Department of Neurosurgery, University of Illinois at Chicago, Chicago, IL 60612, USA; lmcguir1@uic.edu (L.S.M.); fcharbel@uic.edu (F.T.C.)
[2] Richard and Loan Hill Department of Biomedical Engineering, University of Illinois at Chicago, Chicago, IL 60607, USA; mzafar9@uic.edu (M.Z.); rmanwar@uic.edu (R.M.)
* Correspondence: avanaki@uic.edu

Abstract: Due to the high possibility of mechanical damage to the underlying tissues attached to the rat skull during a craniectomy, previously described methods for visualization of the rat brain in vivo are limited to unilateral craniotomies and small cranial windows, often measuring 4–5 mm. Here, we introduce a novel method for producing bilateral craniectomies that encompass frontal, parietal, and temporal bones via sequential thinning of the skull while preserving the dura. This procedure requires the removal of a portion of the temporalis muscle bilaterally, which adds an additional 2–3 mm exposure within the cranial opening. Therefore, while this surgery can be performed in vivo, it is strictly non-survival. By creating large, bilateral craniectomies, this methodology carries several key advantages, such as the opportunity afforded to test innovate imaging modalities that require a larger field of view and also the use of the contralateral hemisphere as a control for neurophysiological studies.

Keywords: bilateral craniectomy; brain imaging; surgery; photoacoustic imaging; optical imaging; cranial window

Citation: McGuire, L.S.; Zafar, M.; Manwar, R.; Charbel, F.T.; Avanaki, K. A Bilateral Craniectomy Technique for In Vivo Photoacoustic Brain Imaging. *Appl. Sci.* **2023**, *13*, 12951. https://doi.org/10.3390/app132312951

Academic Editor: Vladislav Toronov

Received: 4 October 2023
Revised: 17 November 2023
Accepted: 27 November 2023
Published: 4 December 2023

1. Introduction

Craniotomy is a method for surgically opening or removing the skull of a subject to expose the brain for experimental procedures. Over the last two decades, a lot of work has been carried out to make craniotomy procedures safer for the subject and easier to implement and to provide better visual aid of the brain. During a craniotomy procedure, a section of the skull is lifted or taken out to reveal the brain underneath. Due to their thin, translucent skulls and less opaque cortical tissue, mouse models are frequently employed to assess the effectiveness of optical brain imaging techniques [1,2]. These features enable sufficient light penetration, making mice a suitable choice for such evaluations [3,4]. Lately, there has been a surge in interest in rat brain imaging, primarily driven by the emergence of transgenic rats. These genetically modified rats offer a valuable platform for investigating the underlying pathophysiology of complex behavioral and cognitive conditions [5]. Rat skulls, however, are much thicker (0.6−1.1 mm in rats versus 0.4–0.7 mm in mice depending on the specific strain of the animal and their age) [6]. Performing surgery on rat skulls to expose the brain presents inherent challenges, including risks of cortical bleeding, exposure of the pial surface to the external environment, inflammation, and potential distortion of the brain tissue and vascular structure due to edema [1]. Moreover, there is a risk of mechanical damage to underlying tissue while drilling through a thicker skull surface. Most of the current craniotomy techniques can only create a small window (~4–5 mm diameter) to expose the brain [7–11], which are limited to unilateral exposure due to the presence of the superior sagittal sinus as a midline structure. Newer models have been devised, involving thinning or excision of the bone flap and the insertion of a transparent cover, enabling prolonged observation of the brain. However, these craniotomies also remain

relatively small, measuring up to 7 mm in size [1,12–17]. As a result of these challenges, the rat craniotomy approach has become limited, impeding the achievement of optimal visualization of cortical structures. This limitation, in turn, restricts the comprehensive understanding of neural processes and may also hinder the complete evaluation of optical brain imaging modalities.

In this study, our aim is to present a comprehensive guide for a new bilateral hemicraniectomy technique in rat models. This innovative method allows for complete exposure and visualization of the rat brain in vivo, utilizing optical imaging techniques. To validate the efficacy of our approach, we employed a photoacoustic microscopy imaging system to capture high-resolution images of the brain region, covering a diameter of 15 mm.

2. Materials and Methods

Six-week-old adult rats (Sprague Dawley, Charles River Laboratories, Wilmington, MA, USA) weighing 300 g were used in this study. The animals were caged under 12:12 day:night cycle with ad libitum food and water before the surgery. The surgical tools (Figure 1) were sterilized before and after the surgical procedure to allow for an aseptic approach. This study was conducted in accordance with the Institutional Animal Care and Use Committee at the University of Illinois at Chicago (protocol number: 23–131, date of approval: renewed in August 2023).

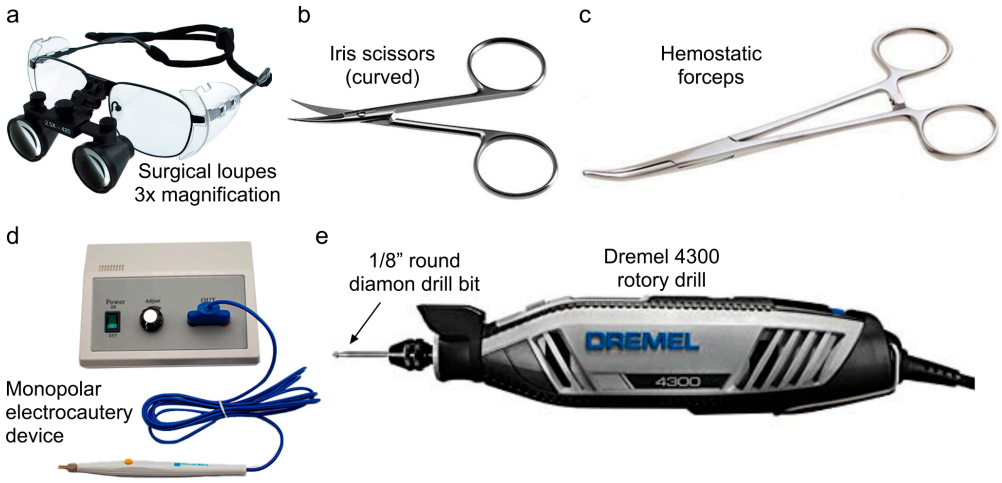

Figure 1. (**a**–**e**) Major surgery equipment used for this study.

2.1. Preparation

1. Rats were first anesthetized using 4% isoflurane inhalation followed by maintenance doses of 2–3% isoflurane during surgery.
2. Adequate depth of anesthesia was confirmed using both toe and tail pinch maneuvers prior to bringing the animal to the surgical platform.
3. The scalp was shaved with hair clippers, and animals were then moved to the stereotactic frame with a heating pad set to normothermic 37 °C to prevent heat loss and hypothermia under anesthesia.
4. The head was immobilized in the stereotactic frame to stabilize the skull during drilling, and the head was positioned in slight extension and without any rotation.
5. Anesthesia continued through a nosecone secured to the frame. The rat was monitored throughout the procedure for respiratory rate and coloration.

2.2. Procedure: Soft Tissue Dissection and Bony Exposure

1. The remainder of the procedure was performed using magnified surgical loupes with 3× magnification (Designs for Vision, Bohemia, NY, USA).
2. The scalp was then opened using scissors in a linear fashion following the midline from immediately posterior to the eyes to the nape of the neck (see Figure 2a).

3. Connective tissue was bluntly freed using gauze, and the skin was reflected laterally using hemostatic forceps during this process (see Figure 2b).
4. Once the connective tissue was fully detached, the scalp was excised in an elliptical fashion.
5. The periosteum was dissected from the bone using a cotton-tipped applicator.
6. Bony hemostasis was achieved using a portable monopolar electrocautery device.
7. The temporalis muscle was then cleared from the underlying temporal bone by detaching the muscle from the temporal ridge using the back of a cotton-tipped applicator or flat dissector.
8. Then, the temporalis muscle was excised sharply with either scissors or 15-blade scalpel. Meticulous hemostasis of the muscle was achieved using a battery-powered, high-temperature, fine-tip Bovie monopolar electrocautery (Bovie Medical Corporation, Clearwater, FL, USA) (see Figure 2c).

These procedures have been summarized in photographs shown in Figure 2.

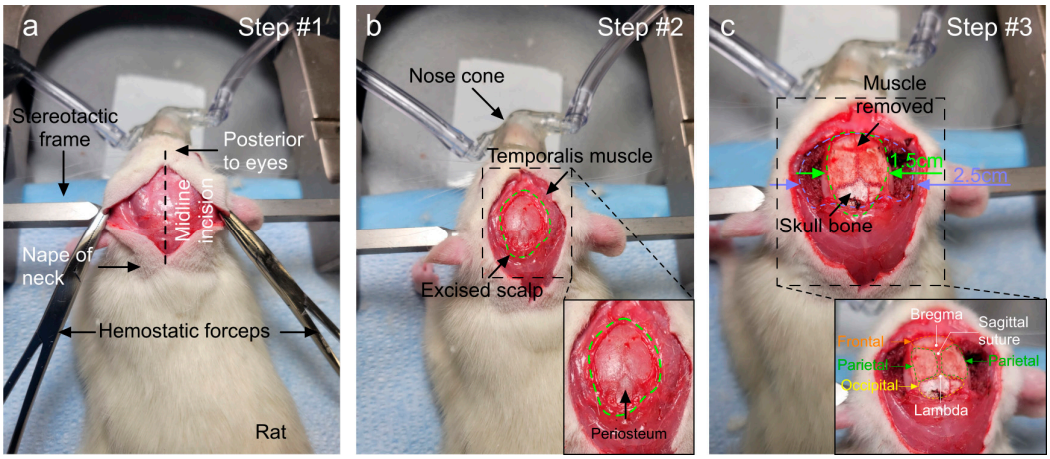

Figure 2. (**a**) Steps of skin incision using scissors with retraction using hemostatic forceps, (**b**) soft tissue dissection to remove connective tissue atop periosteum, followed by elliptical scalp excision to remove forceps, (**c**) temporalis muscle detachment from superior temporal ridge, and then removal using scissors and hemostasis using electrocautery.

2.3. Procedure: Bilateral Craniectomies

1. Once soft tissues were cleared and muscle removed, the following bones and bony landmarks could be seen in full view: bilateral frontal bones, parietal bones, temporal bones, bregma, lambda, and the sagittal suture (see Figures 2c and 3a).
2. The craniotomy commenced using a Dremel 4300 rotary drill with a 225-01 flexible shaft rotary tool attachment.
3. The outer layer of bone was thinned using a 1/8" round engraving drill bit, as the cutting action of the drill allowed for quicker removal of bone.
4. Bone dust was intermittently cleaned from the field with saline solution, and bony hemostasis was achieved as needed using monopolar electrocautery.
5. This thinning process occurred unilaterally by addressing left and right sides separately, encompassing the frontal, parietal, and temporal bones, and sparing the sagittal suture and lambda. The edges of the craniotomy extended from 2–3 mm lateral to the temporal ridge, 2–3 mm anterior to bregma, 0.5–1 mm lateral to sagittal suture, and immediately anterior to lambda.
6. Further thinning of the inner layer of bone to the dura was performed using a 1/8" round diamond drill bit, as the rough surface provided additional hemostasis and was less likely to breach the dura.
7. The cranial thinning with the high-speed drill was performed with utmost caution and precision to avoid injury to the cortical surface and surrounding structures.

8. Once the bilateral craniectomies had been completed through this thinning process, the sagittal suture was addressed, carefully thinning this bone using the 1/8″ round diamond drill bit but leaving the inner layer of bone intact to protect the underlying superior sagittal sinus (see Figure 3b).

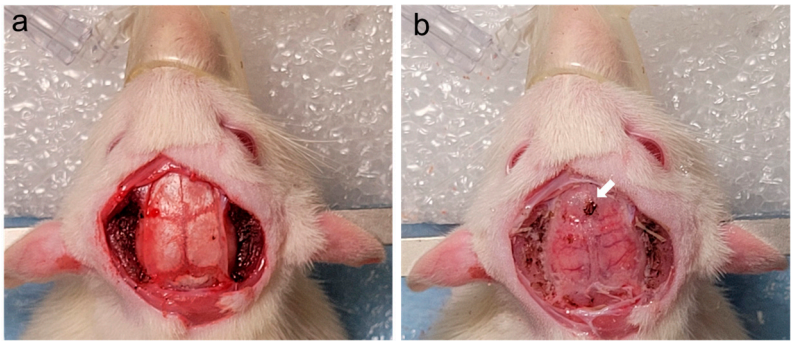

Figure 3. Images of rat's brain (**a**) before and (**b**) after bilateral craniectomies. White arrow on (**b**) indicates a burn mark achieved with hemostatis, described in detail in Section 2.4.

2.4. Procedure: Brain Visualization

After completion of the surgery, the animal was carefully removed from the stereotactic frame, maintaining anesthetic with the nosecone, and transferred to the imaging platform for the experimental phase (see Figure 4).

If this procedure lasts for more than 2–3 h, hydration with subcutaneous injection of saline would be recommended. In our experience, this technique lasted 1–2 h to perform the bilateral craniectomies and an additional 30 min to 1 h for the imaging procedure.

Once the bilateral craniectomy was completed, we imaged the brain of the rat in vivo using optical resolution photoacoustic imaging (OR-PAM). The picture of the setup is shown in Figure 4a. In the OR-PAM system, a 532 nm Nd-YAG laser (VPGL-G-20, V-gen, Tel Aviv, Israel) was used as the optical illumination source with pulse repetition rate of up to 700 KHz.

In the imaging system, the laser light was first passed through iris to achieve spatial filtering and focused on the 2-D galvanometer (GVS 202-2D, Thorlabs, Newton, MA, USA) through a combination of two 90° reflective mirrors (MPD019-G01, Thorlabs, Newton, MA, USA). The XY mirrors in the galvanometer were operated by amplitude and varying sinusoidal phase signals to create a spiral scanning pattern, which is later focused onto the imaging object (rat's brain) using a 10 cm focal length scanning lens (FTH100-1064, Thorlabs, Newton, NJ, USA). The animal's head was placed beneath a homemade water tank with optical transparent bottom covered with saran wrap. The animal's head was pushed up against the bottom saran wrap, and ultrasound gel was applied in between to avoid any air gaps. The PA signals generated upon irradiation of focused laser light were detected using a commercial, wideband ultrasonic transducer (C306, Olympus NDT; central frequency: 2.25 MHz; −6 dB bandwidth 66%). The ultrasonic transducer was positioned inside a water bath at a 30-degree angle (an optimized location for maximum sensitivity) and a distance of 40 mm from the imaging target. We utilized a variable gain voltage amplifier, specifically, the Model 351 A (Analog Modules Inc., Longwood, FL, USA), which is capable of achieving a maximum gain of 80 dB, to amplify the detected PA signals. Subsequently, the signals were captured at a sampling rate of 100 mega samples per second (MS/s) employing a data acquisition device with four channels (CSE1642, GaGe by Vitrek, Lockport, IL, USA). An area of 1.5 cm diameter was imaged at the frame rate of 1.25 Hz and lateral resolution of 48 µm. Details of the system are mentioned in our previous works [18–20].

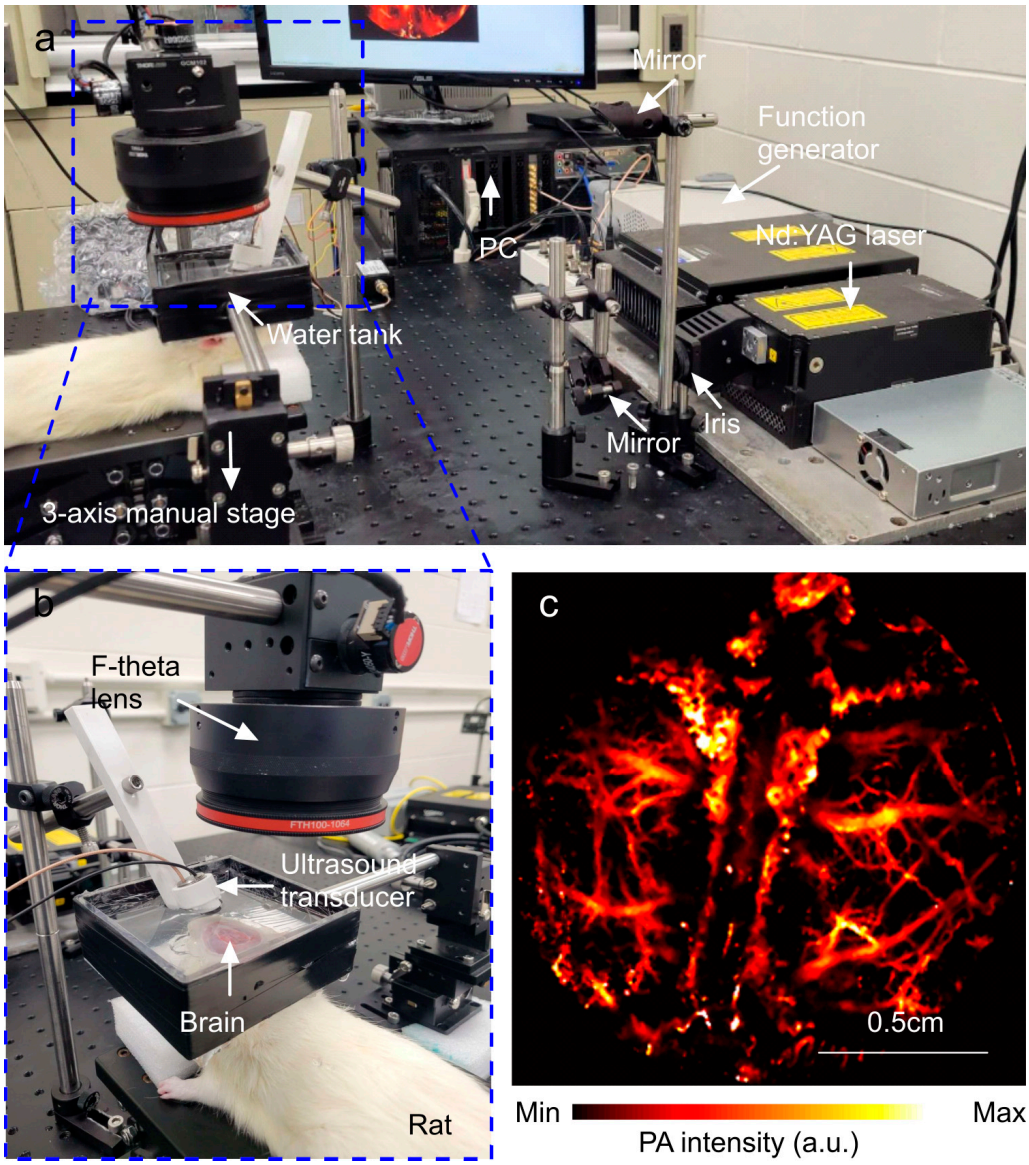

Figure 4. (**a**) Experimental setup of the laser scanning OR-PAM system for rat brain imaging. (**b**) Zoomed-in inset (different angle) enclosed by blue dashed box in (**a**). (**c**) Photoacoustic microscopy image of the rat brain when the scalp and skull are both removed.

2.5. Hemostasis

In this procedure, hemostasis is crucial at every step. Hemostasis is important for several reasons. First, adequate visualization to perform the surgery requires a bloodless field to see each layer of tissue clearly. Second, to best test the imaging modality, blood product should not interfere with testing the technology, and thus, the surgeon must irrigate the field regularly and pause promptly for hemostasis. Third, due to the small blood volume of the animal overall, blood loss can impact the survival of the animal through the surgery, and although it is not a survival surgery itself, the animal is expected to survive the procedure to allow in vivo imaging. Significant blood loss can cause coagulopathy in a process such as disseminated intravascular coagulation, which can exacerbate issues with hemostasis.

Several key instruments can assist with hemostasis: in this method, a monopolar electrocautery unit and soldering iron were implemented, but bipolar electrocautery could be effective, if available. Monopolar electrocautery with a fine tip could be used for scalp, periosteal, bony, or meningeal bleeding. The soldering iron offered more powerful cautery

of the temporalis muscle, especially as a portion of the muscle required resection for this technique. Other agents, such as hydrogen peroxide, are not recommended for this model, although they are effective in general. If hydrogen peroxide encounters the dura or brain tissue, it can be destructive and difficult to control. In addition, the selection of the drill bit was similarly influenced by the goal of hemostasis. While drilling the outer table of bone could be completed with a round cutting drill bit, the inner table was thinned and removed using a diamond drill bit. The cutting drill bit is faster at clearing bone, but the diamond drill bit offers some hemostatic properties and is less likely to injure the dura.

3. Discussion

The rat's skull, like the human skull, is a dense and acoustically heterogeneous structure. When photoacoustic waves pass through the skull, they can undergo scattering, reflection, and refraction (altogether referred to as skull aberration) due to the varying acoustic properties of the skull material. These aberrations can distort the photoacoustic signals and, in turn, can result in blurring, misalignment, or other artifacts in the reconstructed images and eventually make it more challenging to accurately visualize and locate specific brain structures or abnormalities. Many existing craniotomy methods are restricted because of their ability to provide only a limited view of the brain, typically allowing for unilateral exposure due to the presence of the midline superior sagittal sinus. More recent approaches have been developed that involve thinning or removing a section of the bone flap and replacing it with a transparent cover, enabling extended observation of the brain. Nonetheless, these craniotomies still offer relatively limited access. In this study, we presented a feasible approach for a novel bilateral hemicraniectomy technique in rat models, facilitating comprehensive exposure of the rat brain in vivo.

Three primary goals were outlined prior to developing this method: first, maintain a bloodless field to minimize interference of the blood product with the imaging modality; second, preserve normal brain tissue architecture during the craniotomy; and third, create a large cranial window of approximately 1.5 cm to produce an adequate window for the device. In the development of this method, several techniques were attempted to satisfy these goals. One alternative method involved producing troughs with the drill to create a circular cranial flap to subsequently remove en bloc [1]. However, the dura was not consistently preserved in this process, and injury to the cortical surface near the troughs was observed. The sequential thinning process described above resulted in the least trauma to the cortical surface and the most reliable results, and by fully removing the bone over the bilateral cortices but keeping the dura intact, brain injury was minimized not only during the drilling but also during the photoacoustic imaging conducted in this study. While the dura could be removed delicately, it was purposefully kept intact in this method to protect the cortex during brain imaging; as the platform for photoacoustic imaging is lowered, it can be traumatic itself, and the dura helped reduce this injury. Additionally, in this method, to maximize visualization, bilateral exposure was required, but crossing the superior sagittal sinus posed a challenge. Fully removing the bone over the sinus invariably resulted in trauma to this structure, whether minor or major. Thus, the outer table of bone overlying the sinus, which corresponded to the sagittal suture, was removed, but importantly, the inner table of bone was kept intact in this thin strip.

The technique described here differs considerably to other cranial exposures in the literature. In models of traumatic brain injury in the rat, both controlled cortical impact and water percussion injury models involve the use of a trephine to produce a 4–5 mm craniectomy, through which the injury is produced. In the water percussion injury model, midline and lateral craniotomies have been illustrated, whereby the dura is exposed, and then a female Luer lock is cemented in place, allowing for the delivery of a pressure pulse from a column of fluid to induce trauma [8–11]. In the controlled cortical impact model, the mechanism of injury differs: a piston generates the traumatic injury through direct mechanical force on an exposed brain [11]. These models suit the purpose of creating a cranial window to deliver the injury to a focal portion of the cortex, protecting the

surrounding brain with an intact cranial window and allowing for animal survival for later experiments.

More recently, models for longitudinal examination of the cortical surface in rodents have been developed. Several studies in mice have described thinning the skull and adding a glass coverslip over the thinned region or dura for permanent access to the brain for visualization [11]. In rats, similarly, multiple studies have shown the success of implanting a chronic cranial window to allow two-photon fluorescence microscopy, eletrophysiological studies, and functional assessments for several weeks after surgery [1,21,22]. For instance, Koletar et al. detailed the production of a 6 mm craniotomy with the removal of dura and with a glass coverslip implant in the rat, so that repeat assessments with neurovascular function via two-photon fluorescence microscopy could be performed over 14 weeks [1]. In contrast to these models, the technique described here creates a significantly larger window for visualizing the cerebral cortex. With bilateral removal of parietal, frontal, and temporal bones and thinning of the bone overlying the sagittal suture, a wide view of the bilateral convexities can be achieved. The maximum diameter attained with this procedure depends on the rat size; however, a 1.2–1.5 cm length across the convexity could be achieved with temporalis muscle removal. Thus, some inherent advantages accompany this exposure. First, with bilateral exposure, in vivo comparison to the contralateral hemisphere can be performed, such as observing a local vascular response to peripheral electrophysiological stimuli, and thus creating an internal control. Secondly, this large viewing area can be advantageous in the development of novel imaging modalities, which may have a larger field of view.

Several disadvantages, however, accompany this method, in contrast to other techniques. Other models grant survival of the animal for later or repeated experimentation and visualization. Due to the removal of the bilateral cranial surfaces and the resection of the temporalis muscle, this technique must be implemented in non-survival surgery only; thus, no studies across separate experimental time points can be performed. Likewise, while removing this amount of bone was intentional for the purpose of this experiment, the exposed brain could be vulnerable to injury, and caution must be exercised to ensure that instruments do not inadvertently contact the exposed brain. Experimental designs leaving more of the cranium intact provide inherent protection to the brain, allowing instruments to be stabilized on bone. In addition, the technique, as described, does not involve the removal of the dura, which could potentially limit the visualization of the cortical surface depending on the experimental design. This maneuver was intentional in order to protect the cortical surface, both during the bony removal and in the subsequent imaging.

4. Conclusions

Our proposed technique of bilateral hemicraniectomies in the rat offers an opportunity for researchers to test new imaging modalities in vivo that require a large surface area to complete or an internal control for comparison during experimentation. Current methods remain limited by small, unilateral cranial windows of 4–6 mm, whereas our proposed technique offers 2–3× as much space for bilateral visualization with an exposure of 1.2–1.5 cm. Although this method may be used in vivo, this design is strictly non-survival due to the resection of the temporalis muscle and due to the extent of bone removal to maximize exposure, which represents the main limitation of this design. Modifications of this technique could keep the temporalis muscle intact with a smaller bilateral cranial opening and then replace the calvarium with a clear glass or plastic oval, convex cranioplasty. The fast track of the entire surgical process is demonstrated in Supplementary Video S1.

Supplementary Materials: The Supplementary Video S1 can be downloaded at https://drive.google.com/file/d/1HtJ22nrWfSGc3PjL2Q2uKNLMWdIx0hvj/view, accessed on 26 November 2023.

Author Contributions: Conceptualization, L.S.M., M.Z. and K.A.; methodology, L.S.M. and M.Z.; software, M.Z. and K.A.; validation, L.S.M., M.Z., R.M., F.T.C. and K.A.; formal analysis, L.S.M. and M.Z.; resources, F.T.C. and K.A.; writing—original draft preparation, L.S.M., M.Z. and R.M.; writing—review and editing, L.S.M., M.Z., R.M., F.T.C. and K.A.; visualization, M.Z., R.M. and K.A.; supervision, K.A. All authors have read and agreed to the published version of the manuscript.

Funding: This research was funded by the National Institutes of Health R01EB027769-01 and R01EB028661-01.

Institutional Review Board Statement: The animal study protocol was approved by the Institutional Animal Care and Use Committee (IACUC) (protocol number: 23–131, date of approval: renewed in August 2023) at the University of Illinois at Chicago.

Informed Consent Statement: Not applicable.

Data Availability Statement: Data will be provided upon reasonable request. The data are not publicly available due to confidentiality.

Conflicts of Interest: The authors declare no conflict of interest.

References

1. Koletar, M.M.; Dorr, A.; Brown, M.E.; McLaurin, J.; Stefanovic, B. Refinement of a chronic cranial window implant in the rat for longitudinal in vivo two–photon fluorescence microscopy of neurovascular function. *Sci. Rep.* **2019**, *9*, 5499. [CrossRef]
2. Chen, J.; Lambo, M.E.; Ge, X.; Dearborn, J.T.; Liu, Y.; McCullough, K.B.; Swift, R.G.; Tabachnick, D.R.; Tian, L.; Noguchi, K.; et al. A MYT1L syndrome mouse model recapitulates patient phenotypes and reveals altered brain development due to disrupted neuronal maturation. *Neuron* **2021**, *109*, 3775–3792.e3714. [CrossRef]
3. Francis-Oliveira, J.; Leitzel, O.; Niwa, M. Are the Anterior and Mid-Cingulate Cortices Distinct in Rodents? *Front. Neuroanat.* **2022**, *16*, 914359. [CrossRef] [PubMed]
4. Simmons, D.A.; Lartey, F.M.; Schüler, E.; Rafat, M.; King, G.; Kim, A.; Ko, R.; Semaan, S.; Gonzalez, S.; Jenkins, M.; et al. Reduced cognitive deficits after FLASH irradiation of whole mouse brain are associated with less hippocampal dendritic spine loss and neuroinflammation. *Radiother. Oncol. J. Eur. Soc. Ther. Radiol. Oncol.* **2019**, *139*, 4–10. [CrossRef]
5. Matchynski, J.I.; Manwar, R.; Kratkiewicz, K.J.; Madangopal, R.; Lennon, V.A.; Makki, K.M.; Reppen, A.L.; Woznicki, A.R.; Hope, B.T.; Perrine, S.A.; et al. Direct measurement of neuronal ensemble activity using photoacoustic imaging in the stimulated Fos-LacZ transgenic rat brain: A proof-of-principle study. *Photoacoustics* **2021**, *24*, 100297. [CrossRef]
6. O'Reilly, M.A.; Muller, A.; Hynynen, K. Ultrasound insertion loss of rat parietal bone appears to be proportional to animal mass at submegahertz frequencies. *Ultrasound Med. Biol.* **2011**, *37*, 1930–1937. [CrossRef] [PubMed]
7. Kabadi, S.V.; Hilton, G.D.; Stoica, B.A.; Zapple, D.N.; Faden, A.I. Fluid-percussion-induced traumatic brain injury model in rats. *Nat. Protoc.* **2010**, *5*, 1552–1563. [CrossRef] [PubMed]
8. Dixon, C.E.; Lyeth, B.G.; Povlishock, J.T.; Findling, R.L.; Hamm, R.J.; Marmarou, A.; Young, H.F.; Hayes, R.L. A fluid percussion model of experimental brain injury in the rat. *J. Neurosurg.* **1987**, *67*, 110–119. [CrossRef]
9. McIntosh, T.K.; Noble, L.; Andrews, B.; Faden, A.I. Traumatic brain injury in the rat: Characterization of a midline fluid-percussion model. *Cent. Nerv. Syst. Trauma* **1987**, *4*, 119–134. [CrossRef]
10. McIntosh, T.K.; Vink, R.; Noble, L.; Yamakami, I.; Fernyak, S.; Soares, H.; Faden, A.L. Traumatic brain injury in the rat: Characterization of a lateral fluid-percussion model. *Neuroscience* **1989**, *28*, 233–244. [CrossRef]
11. Dixon, C.E.; Clifton, G.L.; Lighthall, J.W.; Yaghmai, A.A.; Hayes, R.L. A controlled cortical impact model of traumatic brain injury in the rat. *J. Neurosci. Methods* **1991**, *39*, 253–262. [CrossRef] [PubMed]
12. Drew, P.J.; Shih, A.Y.; Driscoll, J.D.; Knutsen, P.M.; Blinder, P.; Davalos, D.; Akassoglou, K.; Tsai, P.S.; Kleinfeld, D. Chronic optical access through a polished and reinforced thinned skull. *Nat. Methods* **2010**, *7*, 981–984. [CrossRef] [PubMed]
13. Shih, A.Y.; Mateo, C.; Drew, P.J.; Tsai, P.S.; Kleinfeld, D. A polished and reinforced thinned-skull window for long-term imaging of the mouse brain. *J. Vis. Exp.* **2012**, *61*, e3742. [CrossRef]
14. Dombeck, D.A.; Khabbaz, A.N.; Collman, F.; Adelman, T.L.; Tank, D.W. Imaging large-scale neural activity with cellular resolution in awake, mobile mice. *Neuron* **2007**, *56*, 43–57. [CrossRef] [PubMed]
15. Mostany, R.; Portera-Cailliau, C. A craniotomy surgery procedure for chronic brain imaging. *J. Vis. Exp.* **2008**, *12*, e680. [CrossRef]
16. Holtmaat, A.; Bonhoeffer, T.; Chow, D.K.; Chuckowree, J.; De Paola, V.; Hofer, S.B.; Hubener, M.; Keck, T.; Knott, G.; Lee, W.C.; et al. Long-term, high-resolution imaging in the mouse neocortex through a chronic cranial window. *Nat. Protoc.* **2009**, *4*, 1128–1144. [CrossRef] [PubMed]
17. Cabrales, P.; Carvalho, L.J. Intravital microscopy of the mouse brain microcirculation using a closed cranial window. *J. Vis. Exp.* **2010**, *45*, e2184. [CrossRef]
18. Zafar, M.; Manwar, R.; Avanaki, K. High-fidelity compression for high-throughput photoacoustic microscopy systems. *J. Biophotonics* **2022**, *15*, e202100350. [CrossRef]

19. Mohsin, Z.; James, I.M.; Rayyan, M.; Seyed, M.R.; Alana, C.C.; Shane, A.P.; Kamran, A. Development of fast photoacoustic microscopy system for small animal brain imaging. In *Photons Plus Ultrasound: Imaging and Sensing*; SPIE: Bellingham, WA, USA, 2021; p. 116424B.
20. Zafar, M.; Manwar, R.; McGuire, L.S.; Charbel, F.T.; Avanaki, K. Ultra-widefield and high-speed spiral laser scanning OR-PAM: System development and characterization. *J. Biophotonics* **2023**, *16*, e202200383. [CrossRef]
21. Heo, C.; Park, H.; Kim, Y.T.; Baeg, E.; Kim, Y.H.; Kim, S.G.; Suh, M. A soft, transparent, freely accessible cranial window for chronic imaging and electrophysiology. *Sci. Rep.* **2016**, *6*, 27818. [CrossRef]
22. Scott, B.B.; Brody, C.D.; Tank, D.W. Cellular resolution functional imaging in behaving rats using voluntary head restraint. *Neuron* **2013**, *80*, 371–384. [CrossRef] [PubMed]